Aust. Met. Mag. 43 (1994) 1–16

Norms of apparent temperature in Australia

Robert G. Steadman
School of Agriculture, La Trobe University, Australia
(Manuscript received May 1993; revised August 1993)

Apparent temperature (AT) describes the combined effect on the typical active human of temperature and humidity; optionally, wind and radiation are taken into account. The apparent-temperature model has been refined, and is applied to a range of Australian climate data to analyse the diurnal and annual pattern of normal effects of vapour pressure, wind speed and extra (solar and sky) radiation, and to combine these into maps and charts of apparent temperature. Results show that dry-bulb temperature sometimes over or underestimates the total impact of climatic norms by 10K. Equations are presented to enable calculation of direct and diffuse solar radiation in a clear sky at any time and place on earth. Sunshine is commonly the greatest modifier of dry-bulb temperature in Australia. Daily AT typically reaches its normal maximum before dry-bulb temperature, but seasonal variation of AT lags. Much of the Australian interior has a more temperate climate than dry-bulb alone would indicate.

Introduction

Apparent temperature is an index used by the meteorological services of, for example, UK (Dixon 1991), NZ (Thompson, personal communication 1988) and USA (Climate Analysis Center 1987) as a temperature-like combined measure of all the climatic variables that affect human comfort and performance (Steadman 1984). Expressing heat stress, cold stress or comfort on a familiar temperature scale makes it easier to communicate than measures such as measured sweat rate or imputed heat flow. In summary, the model consists of a typical human, walking at 1.4 m/s and generating heat of 177 Watts for each square metre of total body surface. Of this surface, 90 per cent undergoes full convective and evaporative heat transfer, while the effective radiating area is 72 per cent of the total (Fanger 1970). All of the person's major defence mechanisms against heat and cold are allowed for, including variation in the coverage and thickness of clothing, as typically worn as a function of temperature. This thickness is taken as the exact amount needed to equate heat loss to heat production in steady-state conditions and has a one-to-one correspondence to apparent temperature. This balance will be quantified later as Eqn 15.

Corresponding author address: Dr R.G. Steadman, School of Agriculture, La Trobe University, Bundoora, Victoria 3083, Australia.

Heat transfer basis of apparent temperature

This section summarises previous work (Steadman 1979a,b; 1984) and stresses changes made subsequently to make the equations more realistic, accurate and easily computed.

Of the total heat loss, 177 W/m^2, an amount $25-0.23\ T_a-3\ P_a$ is due to heat and moisture exchange in breathing. See the Appendix for an explanation of symbols. Being independent of wind speed and extra radiation, it is normally computed first when those two variables are being examined. It is subtracted from the total heat loss (or production) to give the total heat loss through the skin,

$$Q_v = 152 + 0.23\ T_a + 3\ P_a \qquad \ldots 1$$

A fraction ϕ_2 of the skin is taken as covered by clothing having a thickness d_f, while the remainder is bare. The present model recognises that for reasons of modesty or decoration, some clothing is worn at any temperature, with the body's own defence mechanisms, such as vasodilation and sweating, offsetting the effect of thermally needless clothing. Many studies of human biometeorology ignore clothing; others assume that it uniformly covers the whole body. In practice, the area of skin covered increases with the clothing thickness, and an empirical fit to human observations in a wide range of climates gives

$$1-\phi_2 = \exp(-11 d_f) \quad \ldots 2$$

Examples are given in Table 2.

Similar observation shows a universal relationship

$$R_f = (14 R_s)^3 \quad \ldots 3$$

for the clothed part. A derivative of this, because $R_s \sim 0.04$ m^2 K/W, is that clothing resistance increases about 12 times as fast as the body's skin resistance, i.e., vasoconstriction alone accounts for only a small part of the body's defence against cold. A value of $R_f = 0.155$ m^2 K/W corresponds to one clo, and 0.100 m^2 K/W to one tog.

Based on information which confounded mass loss due to sweating with that due to breathing, the skin's resistance to moisture transfer was previously (Steadman 1979a,b) underestimated, and some results at high humidities ($P_a > 3.5$ kPa) had to be discarded because the skin relative humidity appeared to exceed 90 per cent. The corrected and more versatile relationship for estimating the person's average resistance to moisture transfer is

$$Z_s = (13\ R_s)^4 \quad \ldots 4$$

The person's primary thermoregulatory mechanism is to allow the core temperature to rise, or fall, triggering the other mechanisms. The clothed person is necessarily warmer than the near-naked subjects on which the present model is based, giving a body temperature that rises as the skin's resistance falls, from the work of Leithead and Lind (1964), as

$$T_b = 33.8 + 1/(7R_s) \quad \ldots 5$$

The body is never at saturation vapour pressure, as many indices suppose, but at about 90 per cent RH (Buettner 1963). A fit to the curve of 90 per cent of saturation vapour pressure in the range 35° to 39.5°C gives

$$P_b = \exp((T_b - 6)/18) \quad \ldots 6$$

Improving on previous work, the 1993 model of apparent temperature recognises the isothermal expansion of evaporated sweat at the generally unsaturated skin. The amount of heat so abstracted is an order of magnitude lower than that due to the phase change, but, being relatively great at lower skin relative humidities, which are as low as 0.35 in Australian conditions, it reveals an appreciable part of the effect of humidity on apparent temperature. Integration of the Clausius-Clapeyron equation for water vapour having a gas constant of 467 Pa m^3/K kg shows a heat loss corresponding to

$$\ln(1/\varepsilon_s)/17 \text{ K/kPa} \quad \ldots 7$$

abbreviated to a humidity function $f(\varepsilon_s)$ for the bare parts and $f(\varepsilon'_s)$ for the clothed parts of the skin. If $\varepsilon_s = 1$, as on a wet-bulb, this effect is zero. When combined with the latent heat of vaporisation this gives an evaporative heat loss of

$$(1 + f(\varepsilon_s))\ (P_b - P_a)/(Z_s + Z_a) \text{ (bare)}$$
$$\text{and } (1 + f(\varepsilon'_s))\ (P_b - P_a)/(Z_s + Z_f + Z_a') \text{ (clothed)}$$

If evaporation occurs at the skin, a fraction $(R_f + R_a')/(R_s + R_f + R_a')$ of this heat loss is taken from the body, the remainder from the surrounding air. The efficiency of evaporation is given by

$$(1 + f(\varepsilon_s'))\ (R_f + R_a')/(R_s + R_f + R_a') \quad \ldots 8$$

where $R_f = 0$ on the bare parts. This efficiency is near 80 per cent as distinct from the 100 per cent which is often assumed in the literature. If the mean skin humidity exceeds 90 per cent, some dripping may occur, lowering efficiency further and multiplying it by a factor

$$1 - 0.5 \exp(-6.6\ (1 - \phi_6)) \quad \ldots 9$$

where ϕ_6, the supposed skin wetness, is lower than the relative skin humidity of the apparent-temperature model (International Organisation for Standardisation 1972).

Because the present model is walking outdoors, the skin humidity is below 90 per cent in all scenarios of Australian norms, so that Eqn 9 is not used in this work.

The clothing thickness d_f is expressed in units of resistance (R_f) to facilitate its derivation from the two environmental variables, temperature and wind speed, that most affect surface resistance. Reflecting the improved wind-resistant fabrics now available, the required thickness d_f is given by

$$d_f = 0.01\ R_f\ (w + 90)\ (1 + (T_a + Q_g\ R_a')/750) \quad \ldots 10$$

The surface resistance R_a' is the reciprocal of the sum of convective and radiative heat-transfer coefficients, the former being a function of wind speed (Table 1) and the latter of temperature,

$$h_r = 3.3 + (T_a + Q_g\ R_a)/28$$
$$R_a = 1/(h_r + h_c)$$

For convenience in computation, the variable $w = h_c + 0.5$ is introduced, giving

$$h_r + h_c = w + (T_a + Q_g\ R_a)/28 + 2.8 \quad \ldots 11$$

Because of confusion in the literature between wind speeds encountered by the person on the ground and by the ten-metre anemometer, attention is drawn to the values in Table 1. These show that the former speed is usually barely half of the latter. For a typical person generating 177 W/m^2 or about 300 W, quoted heat gains exceeding 400 W into a typical person having a heat capacity of 300 kJ/K, if they happened, would cause a temperature increase of 1K every 8 minutes, causing death within an hour. Such conclusions indicate the need for refinements to some conventional simplifications and assumptions.

Because of the increase in body diameter and hence surface area occasioned by donning insulative clothing, the surface resistance, referred to the body's surface, is effectively reduced and, for the clothed parts, is given by

$$R_a' = R_a/(1 + 0.5\ d_f) \qquad \ldots 12$$

Surface resistance to moisture transfer is likewise given by:

$$Z_a = 1/(16w) \text{ for the bare parts} \qquad \ldots 13$$

and $Z_a' = Z_a/(1 + 0.5\ d_f)$ for the clothed parts ...14

For a person walking in an environment having temperature T_a, vapour pressure P_a, wind speed derivative w and extra radiation Q_g, the determination of apparent temperature begins with an iterative solution of d_f to Eqn 1 and the heat balance equation

$$\begin{aligned} 152 + 0.23\ T_a + 3\ P_a = \\ (1-\phi_2)\ (T_b - T_a - R_a\ Q_g + R_a(P_b - P_a) \\ \{1 + f(\varepsilon_s)\}/(Z_s + Z_a))/(R_s + R_a) \\ + \phi_2\ (T_b - T_a - R_a'\ Q_g + (R_f + R_a')\ (P_b - P_a) \\ \{1 + f\ (\varepsilon_s')\}/(Z_s + Z_f + Z_a'))/(R_s + R_f + R_a') \end{aligned} \qquad \ldots 15$$

where the components are as defined in Eqns 2 to 8 and 10 to 14 and $Z_f = R_f/8$.

At each iteration the difference between the left and right-hand sides is multiplied by $(R_s/15)^{1.6}$ to give a correction that is subtracted from R_s. Trials showed this to provide the fastest versatile convergence. Iterations continue until the two sides agree to within 0.02 W/m^2 or one part in 8000, though other levels of precision can be chosen.

Base conditions: determining apparent temperature

Equation 15 yields the required skin resistance to obtain thermal equilibrium. This has a one-to-one correspondence to the skin's moisture resistance, the body's temperature and vapour pressure, the clothing's thermal resistance and, importantly, the apparent temperature. With the adjustments of Eqn 10 it corresponds approximately to the thickness of clothing and the proportion of the skin surface clothed.

Establishing scales of apparent temperature begins with 'base' conditions in which the effects of wind, humidity and extra radiation are neutral, with both positive and negative deviations possible. Base conditions are described as:

(a) an ambient vapour pressure of
  (i) saturation when $T_a \leqslant -3°C$
  (ii) $0.6 + 0.04\ T_a$ when $-3°C \leqslant T_a \leqslant 26.3°C$
  (iii) $(T_a + 273)/181.4$ when $T_a \geqslant 26.3°C$.
  The last equals a vapour concentration of 12 g/m^3, the standard level maintained in temperate-zone physical testing laboratories.
(b) no wind except that generated by the person's movement;
(c) no extra radiation.

With these three variables set at these values, the base relationship between skin resistance and AT is established over the range $-40°C \leqslant AT \leqslant 50°C$. Following trials to find the briefest equation with good fit for Australian conditions, a curve fit to this relationship having a maximum deviation <0.13 K over the range −5° to 45°C is

$$\begin{aligned} AT = -152.8 - 199.4\ X - 91.52\ X^2 \\ -20.39\ X^3 - 1.656\ X^4 \end{aligned} \qquad \ldots 16$$

where $X = \ln R_f$.

This is programmed at the end of the iterative procedure of Eqn 15 to enable any set of conditions T_a, P_a, v_{10} and Q_g to be analysed and its apparent temperature determined to ±0.1K. This deviation is reached only at AT = 26.3°C, where the curve fit smooths out a discontinuity in the slope of the AT base line.

Extra radiation

This major component of apparent temperature is sometimes a critical 'last straw' in heat stress. It is

Table 1. Convective heat-transfer coefficients as a function of anemometer readings.

v_{10} *(m/s)*	0	2	3	4	5	6	>6
Relative wind speed (m/s)	1.40	1.63	1.97	2.43	2.93	3.45	$0.18 + 0.543v_{10}$
h_c *(W/m^2K)*	9.5	10.5	11.8	13.5	15.2	16.8	$6.7 + 1.69v_{10}$

also the least studied component. It measures the extent to which surroundings supply or remove more radiation than would occur when surrounding radiation temperature equals ambient air temperature. The rate at which it is absorbed at clothing or skin surface, Q_g, is related to mean radiant temperature T_r by

$$Q_g = h_r (T_r - T_a)$$

and to the industrial engineer's operant temperature T_o by

$$Q_g = (h_r + h_c) (T_o - T_a)$$

In meteorology, the extra radiation comes directly or indirectly from the sun and the sky. For a model having absorptivity 0.7 and exchanging 0.72 of possible radiation from its surface, with a projected area factor ϕ_3, direct radiation on the person is related to that on a horizontal actinometer Q_D, by

$$Q_1 = 0.50\ \phi_3\ Q_D/\sin A = 0.50\ \phi_3\ Q_n$$

where a fit of ϕ_3 to Fanger's (1970) data, averaged over all azimuths, is

$$\phi_3 = 0.3014 + 88 \times 10^{-5} A - 746 \times 10^{-7} A^2 + 435 \times 10^{-9} A^3$$

where A is the solar altitude angle.

If the actinometer is receiving diffuse radiation at a rate Q_d, the corresponding radiation absorbed by the person's surface, given a radiative form factor to the sky of 0.4, is

$$Q_2 = Q_d/7$$

For ground that reflects 20 per cent of incident radiation, terrestrial radiation on the person is given by

$$Q_3 = (Q_D + Q_d)/28$$

A curve fit to the author's earlier results on outgoing radiation from the person to the sky gives an improved equation

$$Q = (1 - \phi_4{}^2/2)(T_a + 103) \{1 - \exp(-0.11E) + \exp(-0.11E - 1.1)\} \exp.(-0.10P_a) \quad \ldots 17$$

where ϕ_4 is the fraction of sky covered by cloud.

Two scenarios call for knowledge of the incident direct and diffuse radiation, Q_D and Q_d. The approaches differ in principle but give gratifying agreement.

Cloudless sky with near maximal radiative exchange

This scenario is not directly relevant to normal cloudiness and average insolation but is of interest because maximal radiation is more common than any other level and because it provides 'design' conditions for determining decision rules for human exposure.

Extensive curve fitting to data of the American Society of Heating, Refrigeration and Air Conditioning Engineers (ASHRAE 1977) (which refer to Minneapolis with its great seasonal variation in atmospheric moisture content) with the incorporation of atmospheric absorption properties show that for a solar constant of 1353 W/m^2 the total insolation normal to the sun's rays at any time or place is given on average by

$$Q_n = (1353 - 46 \sin(n - 94))\ f(P_a, E, A) \quad \ldots 18$$

where $f(P_a, E, A)$ is an atmospheric attenuation factor equal to

$$\{(1 - \exp(-0.11E) + \exp(-0.11E - 0.18)) \exp(-0.09\ P_a)\}^{\text{cosec } A}$$

and n is the ordinal number of the day in the year, converted to degrees by ignoring February 29, May 31, July 31, August 31, October 31 and December 31. At present Q_n reaches a maximum near 4 January when the earth makes its closest approach to the sun. This new Eqn 18 is derived from theoretical grounds and an exhaustive study of ASHRAE (1977) and other data. It enables total solar radiation to be determined for any time of year, humidity, solar altitude and elevation, on or above the earth's surface. Fluctuations with a coefficient of variation of about 3 per cent occur due to solar activity, and the term shown as −0.18 varies with atmospheric dust, but only the mean values are relevant in a discussion of norms.

The attenuation factor differs quantitatively from that implicit for long wave radiation in Eqn 17 because of higher transparency of carbon dioxide and water vapour to short wave incoming radiation. Further analysis of the data shows that the fraction of this that is scattered or diffuse is

$$1 - \phi_5 = (0.04 + 0.05\ P_a) \exp(-0.10E)$$

i.e. on a horizontal surface,

$$Q_d = Q_n (0.04 + 0.05\ P_a) \exp(-0.10E) \quad \ldots 19$$

The scattering effect is only roughly proportional to the absorption, i.e. the data correspond only approximately to the Kubelka-Munk law.

Direct insolation on a horizontal surface is given approximately and in general by

$$Q_D = Q_n (1 - \phi_5) \sin A \quad \ldots 20$$

The sun's altitude is given by:

$$\sin A = \sin \delta \sin \lambda + \cos \delta \cos \lambda \cos H$$

where δ, the declination angle, is 23.45 sin (n−79), λ is the latitude and H is the hour angle from solar noon, with each hour corresponding to 15 degrees.

Contour charts of maximum extra radiation for four Australian stations at different latitudes and altitudes are illustrated in Fig. 1. These and other

Fig. 1 Clear-sky extra radiation absorbed by person as a function of time of day and month of year at four Australian stations. (W/m² of skin surface.)

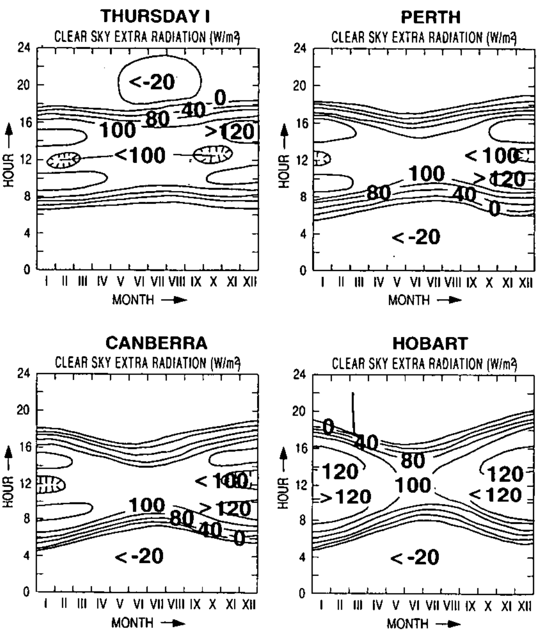

charts correspond to local standard times, except Fig. 9, which refers to solar noon. Examination of Fig. 1 shows some significant similarities. Because the southern summer coincides with the perihelion, seasonal differences in extra radiation exceed those of similar latitudes in the northern hemisphere. The charts, with isotherms at −20, 0, 40, 80, 100 and 120 Watts of absorbed radiation per square metre of total body surface, are calculated from the above equations, and take no account of any effects due to recent reduction of the southern ozone layer. Also significant is that the clear-sky 'design' data shown in Fig. 1, while nominally maximal, can be exceeded. When the sun is nearly overhead, the body's form factor falls to 0.10 to direct radiation, while the corresponding coefficient for diffuse radiation is 0.14. Thus any diffusion of tropical sunlight accompanied by scant atmospheric absorption increases the solar load on the person. This effect requires the sun's altitude angle to be greater than $\sin^{-1}(0.10/0.14) = 46°$. Thin altostratus cloud can have a similar effect by re-radiating diffusely the solar radiation that it absorbs.

Differences between the four stations deserve comment. Average annual radiation on the upright human has less latitudinal variation than on the horizontal actinometer but shows the same trend, with noticeable winter attenuation at Hobart's latitude. The effects of humidity and especially elevation on incoming and outgoing radiation tend to cancel out, making the nett radiation almost independent of altitude, and largely accounting for the similarity in the clear-sky charts for Perth and Canberra. The two times when the sun is nearly overhead are evident in the Thursday Island chart. At tropical coastal stations like Thursday Island, atmospheric moisture reduces the outgoing radiation, which falls to −20 W/m² only on warm dry-season evenings. That this type of radiation depends on surface temperature helps account for the slightly higher peak of nett radiation in the mornings, typically at about 9 am solar time in summer, then a secondary peak near 3 pm, but with a single maximum at solar noon in winter. Expressed in terms of solar altitude, at any season or place, clear-sky nett radiation reaches zero near $A = 6°$ and its maximum near 40°.

Solar noon precedes local standard time by the sum of the distance in degrees by which the station is east of its time-zone meridian and the 'equation of time' which, by the author's Fourier analysis, is given, with a standard deviation of 0.15, as

$$-1.73 \sin n - 0.76 \cos 2n - 2.54 \sin 2n$$

degrees of longitude.

Normal average extra radiation

This was generally derived from hourly means of total and diffuse radiation. Where the actinometer was at some distance from the other recording instruments, ASHRAE (1977) tables were used to correct readings with respect to both longitude (i.e. time) and latitude effects. This especially applies to adjusting radiation data of Williamstown, NSW, to Sydney data for temperature, humidity and wind. The adjusted data, where comparable, are close to those of Spencer (1975).

Because not all 25 stations had hourly radiation data, but all had daily totals shown on maps (Bureau of Meteorology 1982), the required noon norms of both direct and diffuse radiation were derived as follows. ASHRAE formulas for the same latitude (with solar declination reversed for the southern hemisphere) were used to calculate noon intensities and daily totals of both Q_D and Q_d by summing at 40-minute intervals. These were compared with observed daily totals and the noon intensities were determined by proportion.

Applications and simple computing formulas: levels of apparent temperature and their effects

Various indices have been used to estimate the effects of humidity, wind or extra radiation (occasionally two of these, such as the wet-bulb globe thermometer temperature). If the researcher's interest is limited to temperature and humidity, as sometimes happens in summer, the combination is expressed as 'indoor apparent temperature', AT_p, and is obtained by solving Eqn 15 and its antecedents with $v_{10}=Q_g=0$. The effect of humidity is given by AT_p-T_a and is illustrated in Fig. 2.

The dotted envelope of Fig. 2 encompasses climatic conditions found 95 per cent of the time, population weighted, across Australia. The 'shade' apparent temperature AT_{pv} takes account also of wind, with Q_g still set at zero.

To assist in estimating multiple apparent temperatures, especially in forecasting, curve fitting was applied to 30 sets of data, many of them extreme values, giving

$$AT_p = 0.89\ T_a + 3.82\ P_a - 2.56 \qquad \ldots 21$$

With a residual standard deviation of 0.86K, this approximation provides convenience at the price of lost accuracy. In the area within the envelope of Fig. 2, this standard deviation falls to 0.5K.

The wind-chill effect is $AT_{pv}-AT_p$, and is illustrated in Fig. 3 for the special case of $v_{10}=10$ m/s. Because wind-chill, i.e., $T_{pv}-T_p$, is not exactly proportional to the anemometer wind speed, its calculation by proportion from Fig. 3 is accurate to within one per cent only if $6<v_{10}<14$ m/s. In general, a refined version of Table 1 is more reliable and was used in the present work. Of interest in Fig. 3 is a seldom encountered zone of hot dry conditions where wind has a warming effect. A least-squares fit to Australian results is:

$$AT_{pv} = T_a + 3.30\ P_a - 0.70\ v_{10} - 4.00 \qquad \ldots 22$$

This is a more useful approximation than Eqn 21 because of the absence of a single alternative chart corresponding to Fig. 2. The residual standard deviation of 1.20K could be reduced by allowing for non-linearities and interactions among temperature, vapour pressure and wind.

The 'outdoor' apparent temperature AT_{pvg} expresses the sensation of a person walking 'in the sun'. It is often lower than measurements made by exposing a thermometer to sunlight; it also measures negative radiation exposures, as at night. In most applications, $-40<Q_g<130$ W/m^2 and the effect of extra radiation outdoors, $AT_{pvg}-AT_{pv}$, is between -2 and $+8$K. A crude estimate of this effect, which takes no account of clothing, breathing or sweating, is $R_a\ Q_g$ degrees. In practice it is close to the effect that must be estimated more laboriously; the line of exact agreement is shown on Fig. 4, which describes the warming effect when $Q_g=100$ W/m^2 and $v_{10}=0$ (as well as at other combinations such as $Q_g=120$ and $V_{10}=2.3$ m/s).

The extra-radiation effect can be accurately estimated by proportion for other levels of Q_g, even negative levels, but at higher wind speeds, Table 1,

Fig. 2 Effect of humidity (K; solid lines) and apparent temperature (°C) indoors (dashed lines). Dotted envelope encloses 95 per cent of Australian weather.

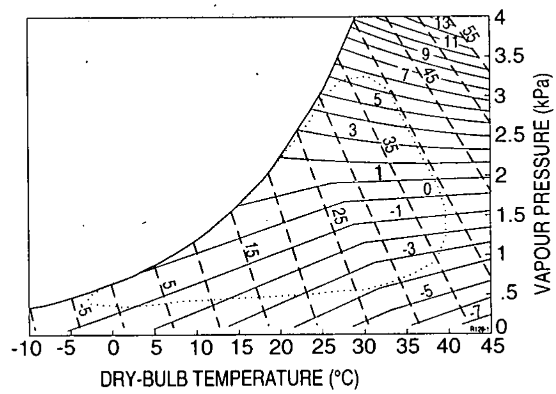

Fig. 3 Effect of a wind of 10 m/s (measured at 10 m height) (K; solid lines) and shade apparent temperature (°C; dashed lines).

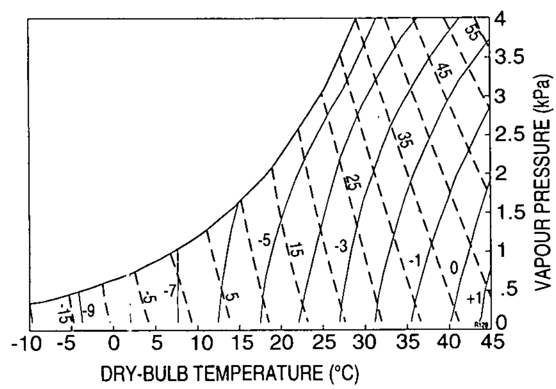

Fig. 4 Effect of extra radiation of 100 W/m² in the absence of wind (K; solid lines) and apparent temperature 'in the sun' (°C; dashed lines).

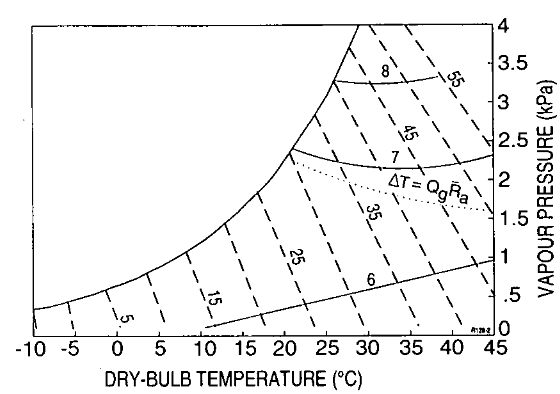

or better, complete computation, is more reliable. The approximation $AT_{pvg} - AT_{pv} = R_a Q_g$ is often better than calculating by proportion wind effects on extra radiation. This effect is almost independent of temperature, despite the wide range of clothing coverage between −10° and 45°C.

The apparent temperature 'in the sun' is given by the approximation

$$AT_{pvg} = T_a + 3.48\ P_a - 0.70\ v_{10} + 0.70\ Q_g/(V_{10} + 10) - 4.25 \quad \ldots 23$$

having a residual standard deviation of 1.21K.

The three effects, of humidity, wind and extra radiation, are worth considering in terms of evitability. Outdoors, humidity cannot be avoided, and the effects shown throughout this paper are felt generally. Wind effects refer to a person who, except for walking on the ground, where the integrated wind speed is reduced almost by half, is exposed like a standard anemometer; most people, especially in cities, experience less effect than shown here. The indicated effect of extra radiation can be reduced, or avoided completely, most of the time.

The results shown here, including the outdoor apparent temperatures, refer to a clothed person fully exposed to all three effects. For many people, the humidity effect may be the only important one. However, sporting and military activities are normally associated with full exposure, for which outdoor apparent temperature is the most reliable measure of thermal safety and comfort.

Maps of apparent temperature

All three levels of apparent temperature were determined for 25 key stations near noon across Australia. For normal conditions, temperature was taken as a weighted mean, in the ratio 3:1, of maximum and minimum temperature. Daily mean vapour pressure was used. Wind speed was taken as 1.2 times the daily mean, whenever noon means were unavailable. The proportion of diffuse radiation at noon was estimated from

$$\phi_5(0) = 1 - \sin A(40) / \{\sin A(40) - \sin A(0) + \sin A(0)/(1 - \phi_5)\}$$

where A(0) is the sun's altitude at noon, A(40) is the sun's altitude after 40 per cent of the solar afternoon has elapsed, i.e., at a median level of radiation, and ϕ_5 is the quoted mean direct proportion of daily global radiation. (If ϕ_5 is unavailable, an approximation is $\phi_5 = 0.9 - \phi_4$.)

Basic meteorological data were obtained from climate summaries, e.g. Bureau of Meteorology (1982). These were supplemented by more specific hourly data kindly supplied by the Bureau of Meteorology (Nydam, personal communication 1986). The techniques of the previous section were applied to these data to process them into the four input parameters T_a, P_a, w and Q_g. Midnight values were not available for Melbourne and were found by interpolation.

Determining the three levels of apparent temperature — of which only the outdoor level 'in the sun' is illustrated here — enabled the separate effects of humidity, wind and extra radiation at solar noon in January and July to be analysed. Results were plotted respectively in Figs 5, 6 and 7. Figure 8 shows the sum of these effects, the amount by which the dry-bulb temperature underestimates the effects on humans. Apparent temperature outdoors is illustrated in Fig. 9. Maps of dry-bulb temperature, the most important component, were used in interpolating apparent temperature between the stations.

Apparent temperature and its effects are higher in January than July except for the shaded areas of Figs 6–8, all of which show a tendency toward seasonal moderation of apparent temperature.

Remarks on the maps of apparent temperature

Figure 5 (humidity effects) illustrates Australia's status as a dry continent, with barely half of the area showing a warming effect of moisture at noon even in January. In the wet season, these affects can be uncomfortably high, with Darwin showing a warming effect comparable with that of other monsoonal climates in the world's tropical zone. Equatorial climates (Thursday Island, Cairns) show considerably less seasonal variation than monsoon climates of similar latitude (Darwin, Broome). Much of the interior shows a dry cooling effect exceeding 1K at all seasons at noon. The zero isotherm for January approximately represents the northern limit of practicable evaporative cooling for buildings.

Wind effects (Fig. 6) have greater local variations than the maps can show, and some of the effects plotted are merely due to site peculiarities of the anemometers, especially at coastal stations. Despite the general observation (Fig. 3) that, for a given wind speed, cooling effect varies seasonally in the opposite direction from ambient temperature, many Australian stations show more cooling due to wind in summer. This effect, which helps temper the climate in real human terms, is illustrated by the shaded parts of the July map. Few other parts of the world show a milder cooling effect for wind in winter than in summer. The shaded area is plotted conservatively, with Melbourne, Canberra, Esperance and Cloncurry showing a difference between January and July noon wind effects of 0.0K.

Fig. 5 Effect of environmental humidity in Australia near solar noon in January and July (K).

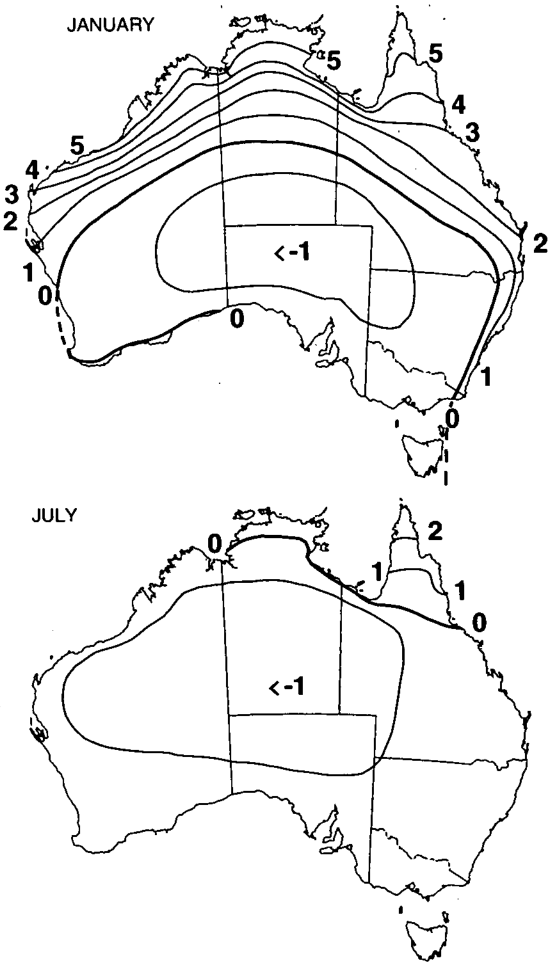

Fig. 6 Effect of full exposure to normal wind in Australia near noon in January and July (K). Shaded areas in Figs 6 to 8 refer to zones where the moderating effect is better than in January.

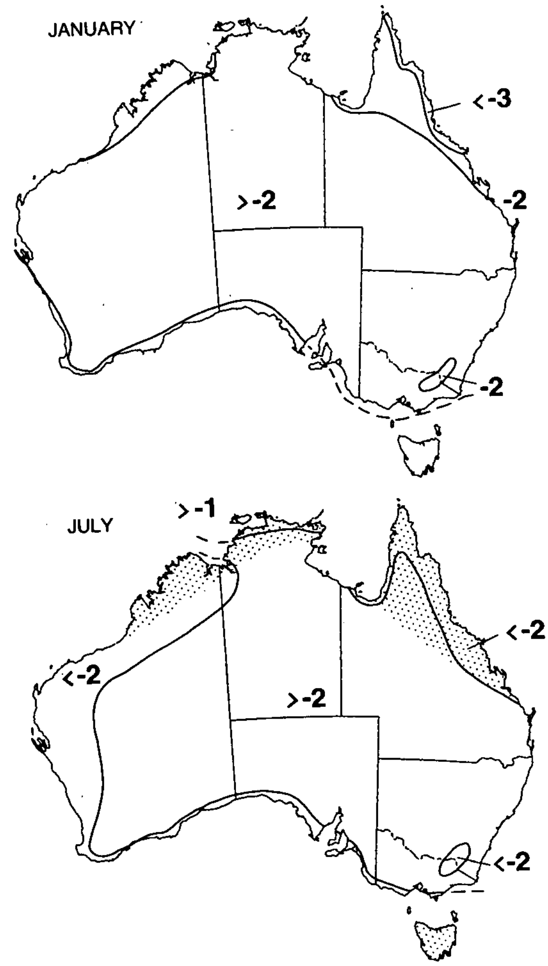

Extra radiation (Fig. 7) is appreciable in most of Australia, though some mesoscale cloudy pockets cannot be shown. Winter cloud in southern and western parts has a greater attenuating effect than does rainy season cloud in the north. This occurs because the winter sunshine is absorbed by a long atmospheric path at low solar altitude, while the tropical sunlight is generally scattered and affects the person as strong diffuse radiation. At all seasons, the outdoor person at noon in most parts of the country is warmed by at least 5K; in the tropics, and in summer elsewhere, this increment is higher before and after solar noon. Over a large part of Australia (the shaded area), the normal noon warming effect of July is greater than in January, chiefly because the winter noon sun projects a greater surface area of the human.

The combination of the three effects is shown in Fig. 8. In the wet season the 'Top End' feels more than 10K hotter than the dry-bulb temperature. At the other extreme, even the noon sun fails to offset the cooling effect of winter wind in some southern regions. In the shaded area the combined July effects exceed those of January; in those places the climate, with little increase of moisture in summer, may be more temperate than dry-bulb data would indicate. Again, this seasonal reversal is rare in the world's temperate zone. Figure 9 is a plot of apparent temperature, taking account of only extensive altitude effects. In all places the

Fig. 7 Effect of full exposure to normal extra radiation in Australia at solar noon in January and July (K).

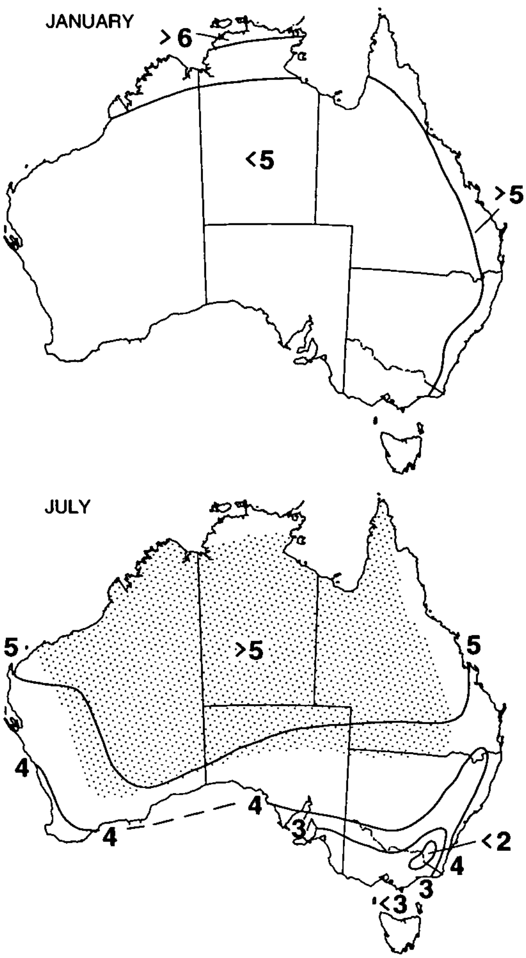

Fig. 8 Sum of effects shown in Figs 5 to 7, i.e. the amount by which dry-bulb temperature underestimates thermal sensation (K).

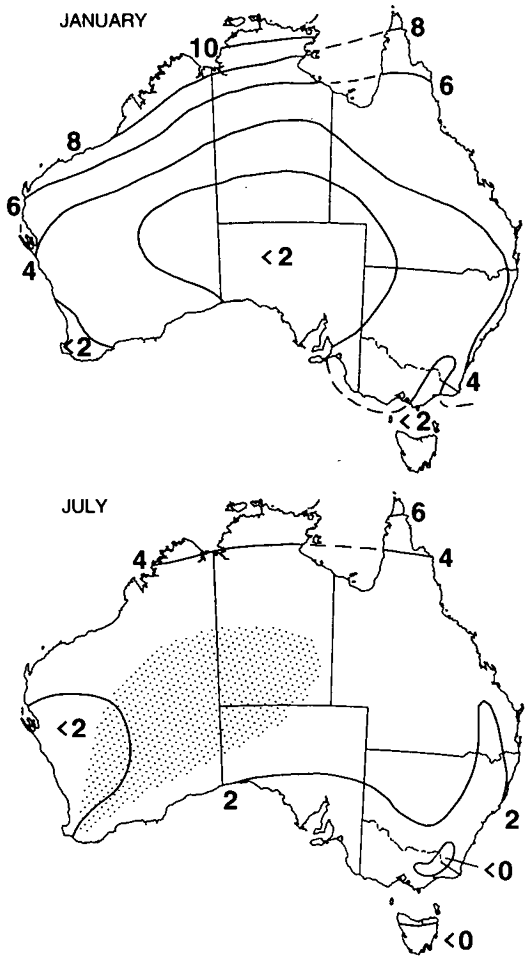

January AT exceeds that of July by at least 5K. As with dry-bulb temperature, latitudinal gradation is steeper in winter than in summer. The hottest norms are below those of central Pakistan (Steadman and Choudhury 1987), the Persian Gulf and South-East Asia.

Other combined measures of thermal comfort

The two most common alternatives are sweat rate and skin humidity because they both change greatly in sultry conditions. Insensitive in cold conditions, they lack versatility as combined measures of the effects of temperature, humidity, wind and extra radiation.

On psychrometric charts analogous to Figs 2–4, the isopleths of sweat rate, whether gross moisture loss or nett cooling effect, are essentially vertical, i.e. they measure temperature but take insufficient account of humidity. On the other hand, skin relative humidity gives almost horizontal lines, nearly independent of temperature. In the presence of extra radiation, skin relative humidity falls slightly. Older, approximate plots of both properties are in the literature, along with the efficiency of evaporation (Steadman and Choudhury 1987, p.19).

Fig. 9 Normal apparent temperature at solar noon in Australia, January and July (°C).

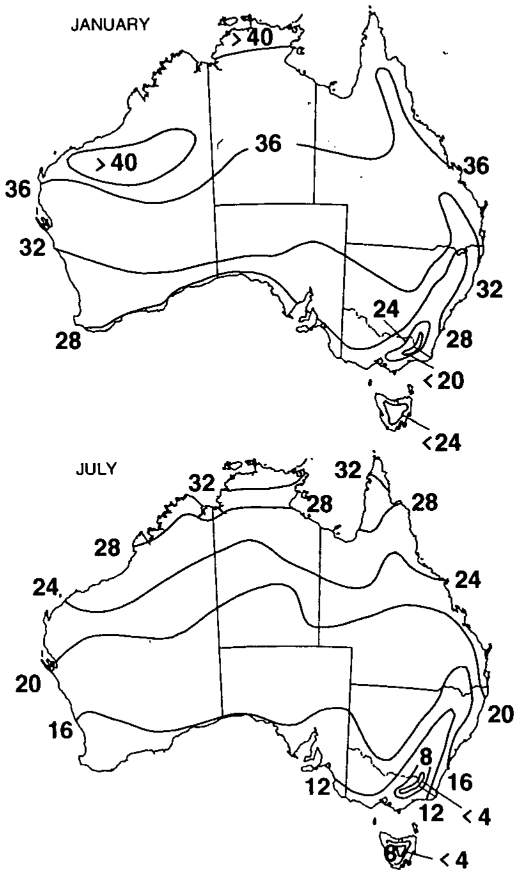

Fig. 10 Seasonal and diurnal variations of normal apparent temperature (°C) and an analysis of effects (K) for Adelaide.

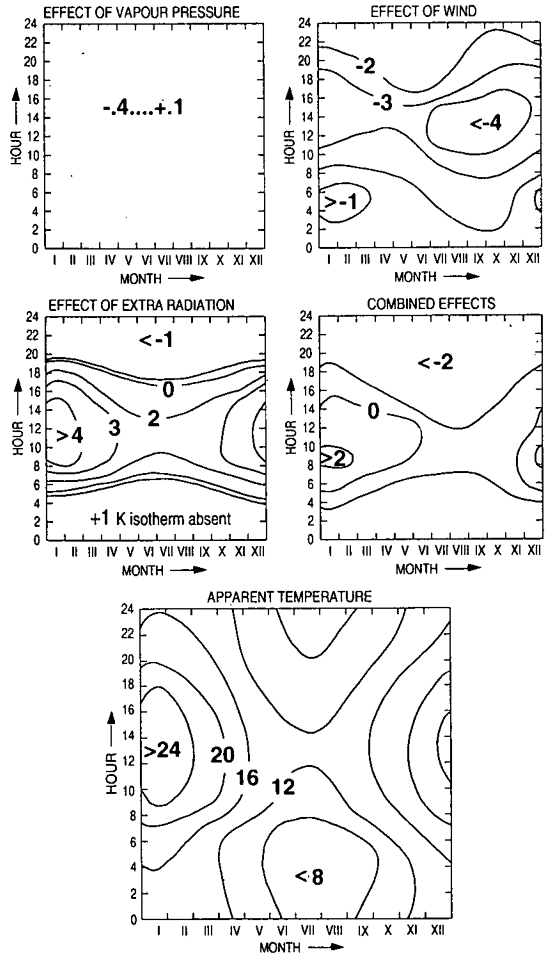

Contour charts of seasonal and diurnal variations

To provide a better picture of seasonal and diurnal variation in major centres, data were processed for nine stations and illustrated in Figs 10 to 18. These include Darwin, Canberra, Alice Springs and the six State capitals. Alice Springs arguably represents almost as much of Australia's area as the eight other population centres combined.

This information was obtained from monthly mean data at three-hourly intervals. As before, the most difficult part was the realistic conversion of direct and diffuse solar radiation from hourly means into solar heat load on the body at exact local times. Calculations of sunrise, sunset and solar noon improved precision. In the absence of cloud, incoming radiation offsets outgoing radiation, i.e., nett radiation Q_g is typically zero about 20 minutes after sunrise and 20 minutes before sunset, longer in high latitude winter. A warming effect of +1K is reached so close to 0 or 2K that the 1K isotherms are omitted from the charts of extra radiation.

Vapour pressure effects are normally slight south of the median line that holds half of Australia's population. At stations where the total range of this effect is less than 1K, there is no attempt to draw a fairly insignificant zero line; only the range of the normal effect is shown. North of Sydney, a strong seasonal pattern in vapour pressure effects is noticeable.

Variation in wind effects generally shows more horizontal isotherms, i.e. the change is more diurnal than seasonal. The cooling effect of wind

Fig. 11 As in Fig. 10 for Alice Springs.

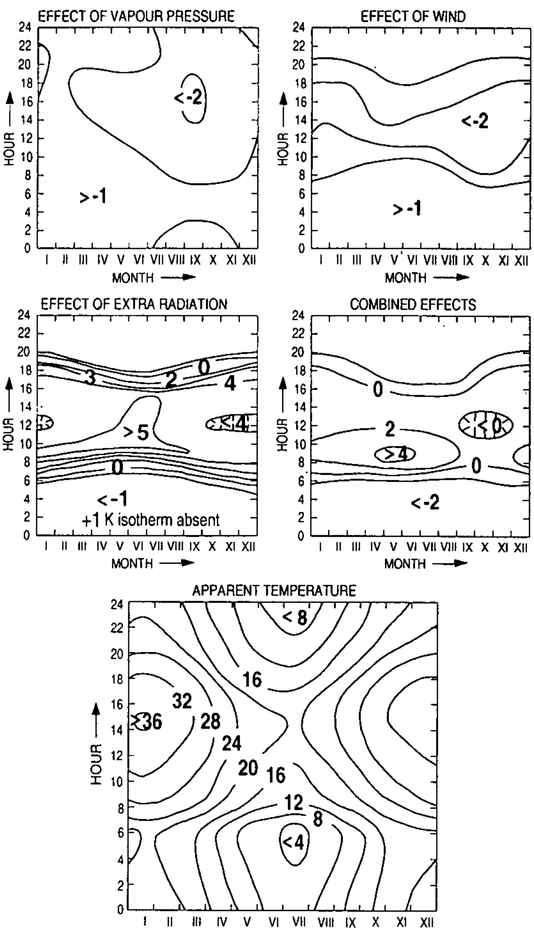

Fig. 12 As in Fig. 10 for Brisbane.

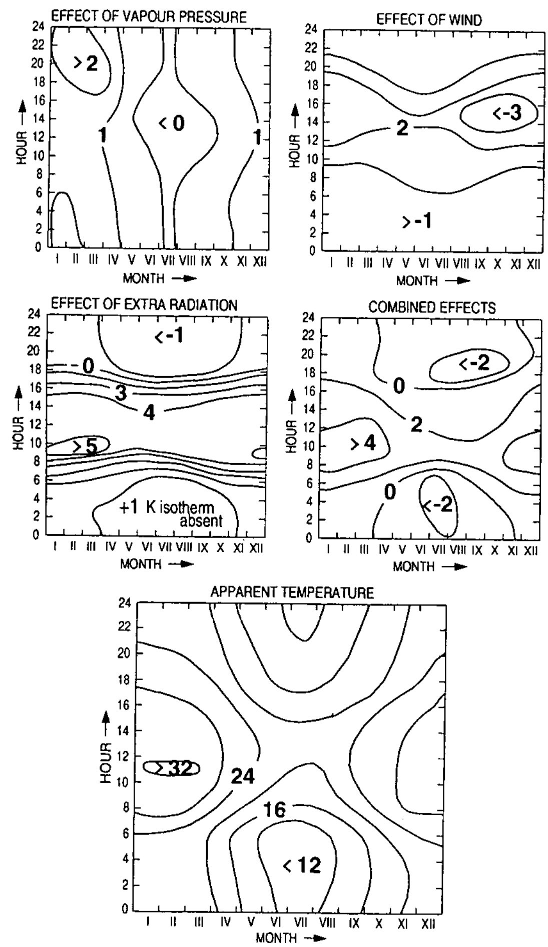

in Australia tends to be greatest (i.e. lowest negative values are shown) on spring afternoons, and least before sunrise in summer. No instances of normal wind warming effects were found.

Extra radiation effects are commonly greater than the two preceding. Synergism with humidity (Fig. 4) makes sunshine oppressive, even when diffused by cloud, in the tropical wet season. Likewise, the time in which the normal effect exceeds 4K is more than twice as great in Brisbane as in Perth, despite similar actinometer readings.

At Darwin, as in most monsoon climates, the humidity effect reaches a seasonal maximum just before the onset of the monsoon. The effect commonly reaches a maximum well before solar noon. Because of afternoon winds, the afternoon peak is lower. The body's lower projected area factor to direct overhead sunshine is noticeable in the plots for the two tropical stations. Outgoing nocturnal radiation tends to be greatest (Eqn 17) in warm dry air.

Combined effects are normally slight at southern centres, the effects of wind and extra radiation roughly balancing during daylight hours. This depends chiefly on latitude, with Darwin's norms seldom below zero, and Hobart and Melbourne seldom above. The combined effect is usually greatest on summer mornings while the sun is still low enough to project a large area of the person. At Alice Springs the seasonal progression of the combined effects opposes that of the dry-bulb temperature, indicating a more temperate climate than dry-bulb alone would indicate.

These norms of combined effects provide a useful approximation in forecasting, by giving a

Fig. 13 As in Fig. 10 for Canberra.

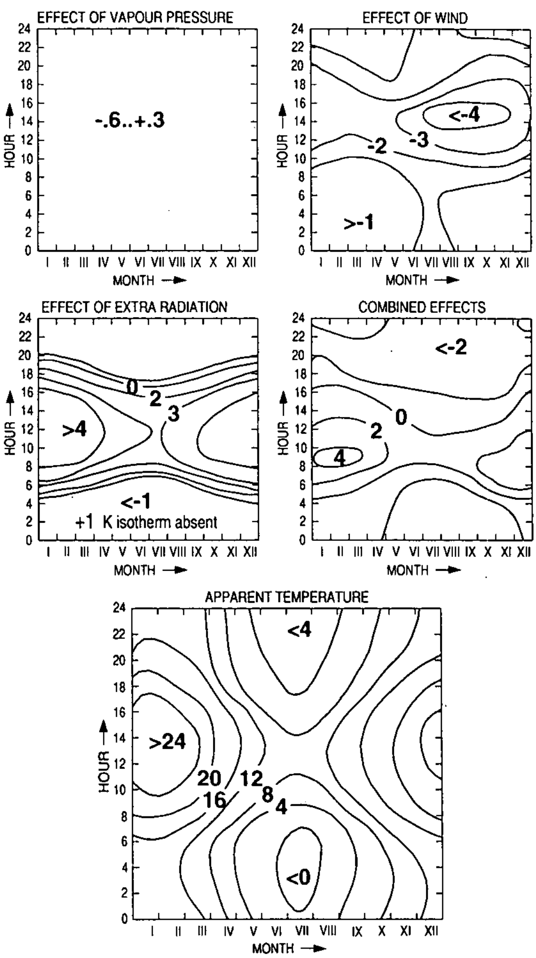

Fig. 14 As in Fig. 10 for Darwin.

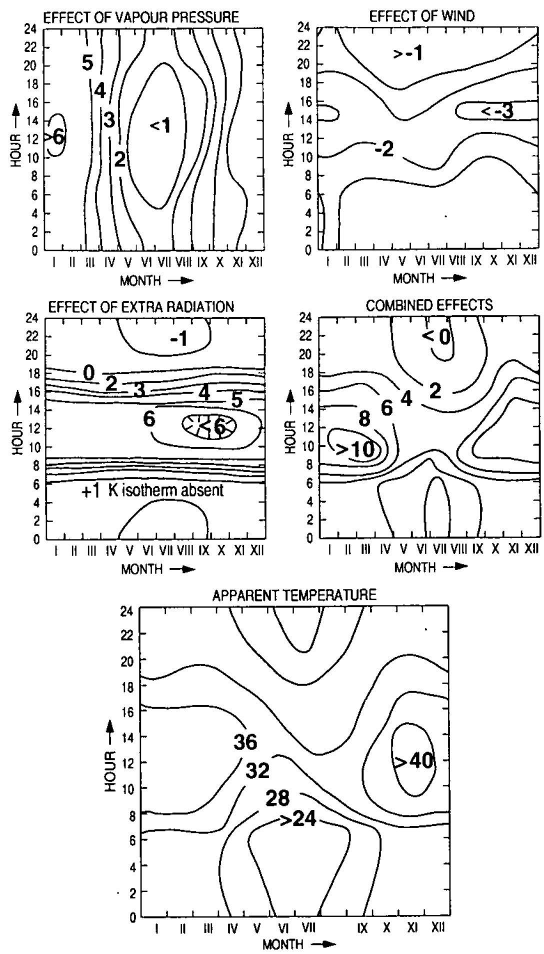

simple adjustment from dry-bulb to apparent temperature. For instance, a forecast maximum dry-bulb of 25°C might be accompanied by predictions of a humidity effect of +1K, a wind cooling effect of −5K and a warming effect of extra radiation reaching 6K. Indoor and shaded outdoor apparent temperatures are not illustrated, only the AT when fully exposed to extra radiation.

Because of lingering summer humidity and lowering solar altitude, the seasonal maximum of AT tends to be a few weeks later than that of dry-bulb temperature, with a shorter delay of the minimum in winter. This is contrasted with the diurnal progression, where the daily maximum of AT precedes that of dry-bulb temperature, sometimes happening before solar noon. The sharp changes in AT near sunrise and sunset are noticeable in some of the contour lines.

This paper is not a medical treatise, but the opinion is offered that outdoor sports and military exercises should not be scheduled when the normal AT in the sun exceeds 35°C and should be suspended when the observed AT exceeds 40°C. The contour charts provide the base for such decisions. Depending on the person's activity and its duration, exposure to AT above 35°C leads to hyperthermia.

Properties corresponding to apparent temperature: clothing requirements

Those characteristics of the model having a one-to-one correspondence with apparent temperature are listed in Table 2 at five-degree intervals.

Fig. 15 As in Fig. 10 for Hobart.

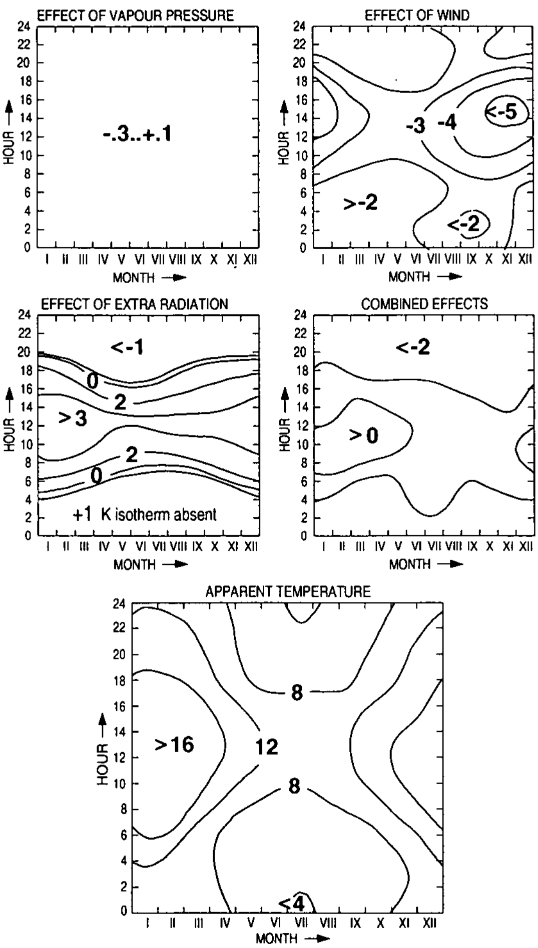

Fig. 16 As in Fig. 10 for Melbourne.

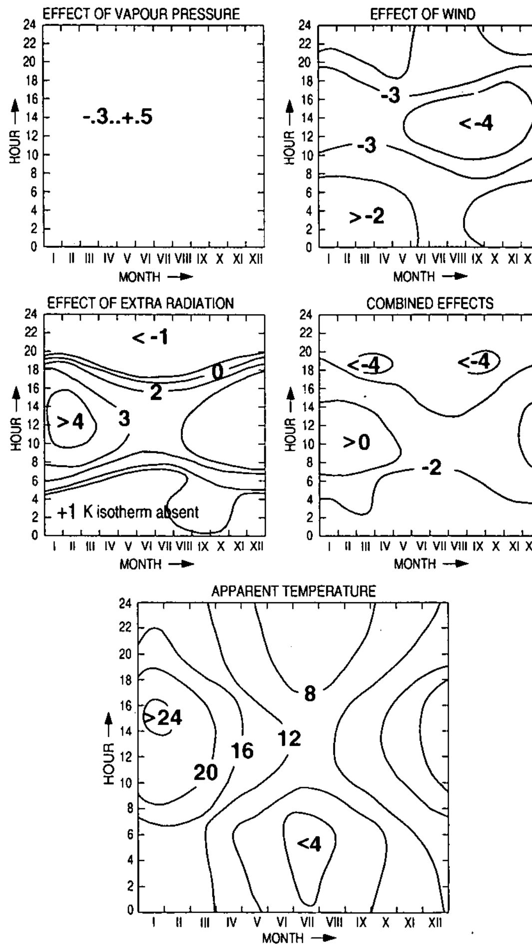

For clothing resistance and the proportion of skin surface clothed, the correspondence is exact only when $0.01\ (w+90)\ (1+(T_a+Q_g\ R_a)/750)=1$, but is close in all conditions. Table 2 shows qualitatively the type of clothes that would be added with each temperature decrement to enable the wearer to approach thermal equilibrium.

The model also provides results of mean skin temperature and humidity; sweat rate and efficiency; and heat losses from clothed and exposed parts. These all vary also with wind speed and extra radiation, and do not lend themselves to the generalisation of Table 2.

Table 2. Properties of the model varying with apparent temperature.

AT	R_s	Z_s	T_b	P_b	ϕ_2	R_f	*Apparel increment*
40	.0255	.0121	39.4	6.39	.395	.0457	Minimal; sun protection as needed
35	.0276	.0165	39.0	6.25	.469	.0575	Short sleeve, shirt and shorts
30	.0299	.0227	38.6	6.11	.552	.0731	Light undershirt
25	.0324	.0314	38.2	5.99	.641	.0931	Cotton-type slacks
20	.0349	.0426	37.9	5.88	.724	.1171	Normal office wear
15	.0374	.0560	37.6	5.79	.794	.1438	Thin or sleeveless sweater
10	.0397	.0709	37.4	5.72	.849	.1716	Sweater; thicker underwear
5	.0418	.0868	37.2	5.67	.889	.1997	Coat and sweater
0	.0436	.1034	37.1	5.62	.918	.2277	Overcoat; wind protection as needed
−5	.0453	.1203	37.0	5.57	.940	.2552	Head insulation; heavier footwear

Fig. 17 As in Fig. 10 for Perth.

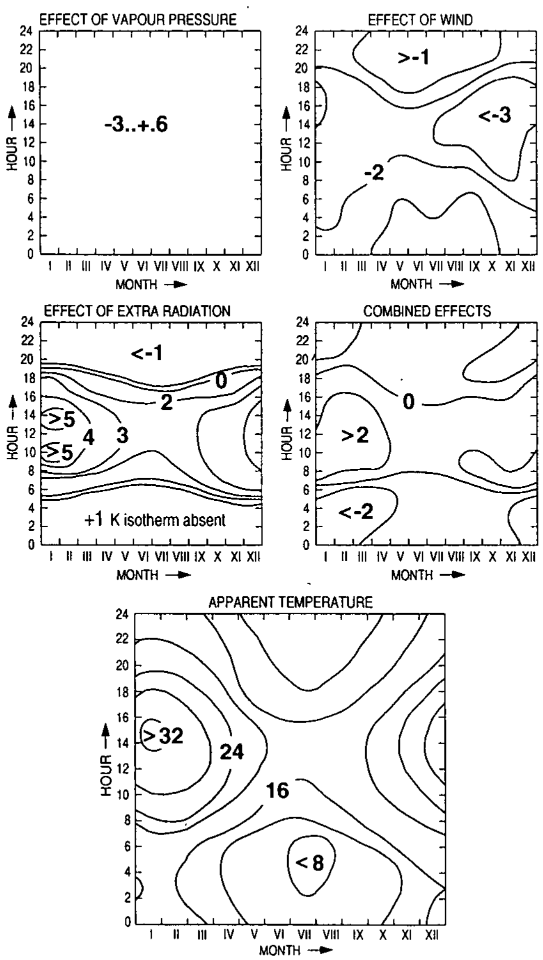

Fig. 18 As in Fig. 10 for Sydney.

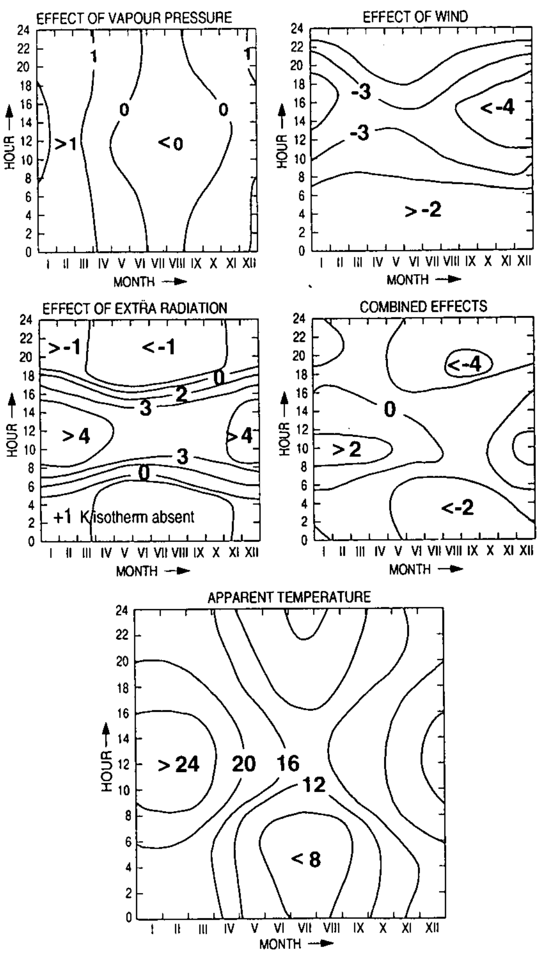

Frequency distribution of apparent temperature

Contour charts, such as Figs 10 to 18, include normal apparent temperature, for persons fully exposed to sunshine, at any time of the day and year. They are misleading in the sense that they only roughly describe temporal distribution and underestimate the incidence of dangerously high and low temperatures.

In other work (Steadman 1980) dry-bulb temperature was shown to be approximately normally distributed with daily means having a standard deviation $s = 0.56 + 1.062\ s_m$, where s_m is the population standard deviation of the twelve monthly mean temperatures (essentially measuring the seasonal variation).

The distribution of dry-bulb temperatures deviates from gaussian only in sultry summer climates where much of the heat is latent, as humidity rises. Thus apparent temperatures can be expected to approximate to a 'normal' distribution more closely than dry-bulb temperatures. The mean and standard deviation s_m of 96 (12 monthly $\times$ 8 daily) normal temperatures were determined for the nine key stations and have been used to estimate cumulative frequencies of AT (Table 3).

With each percentage point corresponding to 88 hours per year, the possibility of exposure to dangerously hot conditions is great in tropical areas, appreciable in many cities. Evidence that such risk can be avoided by 'acclimatisation' is scant, and invariably appears in trials where no control samples were tested, nor double-blind experiments conducted. The risk of heat stress and discomfort arguably exceeds that suggested in some reviews, e.g. Colls and Whitaker (1990, pp. 60–62). In Australian cities, very low apparent temperatures, especially during working hours, are uncommon. But even cities that are physically

Table 3. Frequency distribution of apparent temperature at major stations.

		Adelaide	*Alice Springs*	*Brisbane*	*Canberra*	*Darwin*	*Hobart*	*Melbourne*	*Perth*	*Sydney*
Mean AT	*(°C)*	14.3	19.9	21.0	11.3	31.2	10.7	12.8	17.3	16.2
Standard deviation	*(K)*	6.6	9.9	7.3	8.7	6.2	5.5	6.7	7.6	6.6
Percentage above	*0°*	98	98	>99	91		97	97	99	99
	5°	92	94	98	77		85	88	95	95
	10°	74	84	94	56		55	66	83	83
	15°	54	69	79	34	>99	22	37	62	57
	20°	20	50	56	16	97	5	14	36	28
	25°	5	30	29	6	84	2	4	16	9
	30°	1	15	11	2	58	<1	2	5	3
	35°	<1	6	3	1	27		<1	1	1
	40°		2	1		8				
	45°		<1			1				

frost-free have apparent (wind-chill) temperatures below 0°C at times. Canberra, for instance, 'feels' freezing for about 9 per cent of the time, three times as often as sub-zero dry-bulbs occur.

One of the more striking observations from Table 3 is the relationship between standard deviation and latitude, with some of the most constant AT distributions being at higher latitudes such as Hobart, despite a generally higher variation in dry-bulb temperature. As would be expected from the secondary seasonal influences of humidity, wind and extra radiation, all nine primary stations except Alice Springs showed more variation in AT than in dry-bulb temperature.

Summary

Apparent temperature (AT) describes the combined effect on the typical active human of temperature and humidity; optionally, wind and radiation are taken into account. The apparent temperature model has been refined, and is applied to a range of Australian climate data to analyse the diurnal and annual pattern of normal effects of vapour pressure, wind speed and extra (solar and sky) radiation, and to combine these into maps and charts of apparent temperature. Results show that dry-bulb temperature sometimes over or underestimates the total impact of climatic norms by 10K. Equations are presented to enable calculation of direct and diffuse solar radiation in a clear sky at any time and place on earth. Sunshine is commonly the greatest modifier of dry-bulb temperature in Australia. Daily AT typically reaches its normal maximum before dry-bulb temperature, but seasonal variation of AT lags. Much of the Australian interior has a more temperate climate than dry-bulb alone would indicate.

Acknowledgments

The support of the Bureau of Meteorology staff has been invaluable. Paul Nydam supplied abundant climate data. John Colquhoun (NSW Regional Office) and staff directed typing. Bernard Stokes and Carol Skinner directed redrafting of diagrams.

References

American Society of Heating, Refrigeration and Air-Conditioning Engineers (ASHRAE) 1977. *Handbook of Fundamentals.* ASHRAE, New York.

Buettner, K.J. 1963. The Role of the Skin Barrier Layers. *Proceedings of the Scientific Section of the Toilet Goods Association*, 40, 811.

Bureau of Meteorology 1982. *Climate of Australia.* AGPS, Canberra.

Climate Analysis Center 1987. *Weekly Climate Bulletin.* US National Weather Service.

Colls, K. and Whitaker, R. 1990. *The Australian Weather Book.* Child and Associates, Sydney.

Dixon, J.C. 1991. Wind-Chill. *Weather, 47*, 141–4.

Fanger, P.O. 1970. *Thermal Comfort.* Danish Technical Press, Copenhagen, 244 pp.

International Organization for Standardization (ISO) 1972. Analytical Determination of Thermal Stress. *Draft Standard ISO/DP 7933.* Geneva, 33 pp.

Leithead, C.S. and Lind, A.R. 1964. *Heat Stress and Heat Disorders.* Churchill, London.

Spencer, J.W. 1975. *Sydney Solar Tables.* CSIRO, Australia, 92 pp.

Steadman, R.G. 1979a. The Assessment of Sultriness, Part 1: A Temperature-Humidity Index Based on Human Physiology and Clothing Science. *Jnl appl. Met., 18*, 861–73.

Steadman, R.G. 1979b. Idem, Part 2. Effects of Wind, Extra Radiation and Barometric Pressure on Apparent Temperature. *Jnl appl. Met., 18*, 874–85.

Steadman, R.G. 1980. Minimizing Total Costs of Apparel, Housing and Heating in Maintaining Thermal Comfort Indoors. *J. Consumer Studies and Home Economics, 4*, 223–38.

Steadman, R.G. 1984. A Universal Scale of Apparent Temperature. *Jnl appl. Met., 23*, 1674–87.

Steadman, R.G. and Choudhury, A. 1987. Sultriness in the Indian Sub-continent. *Meteorological Monograph No. 16/1987*, Indian Meteorological Department, 46 pp.

Appendix

Symbols used repeatedly

A Solar altitude (degrees)
d thickness of clothing in R units (m^2K/W)
E elevation above sea level (km)
h heat-transfer coefficient (W/m^2K)
n date (in degrees) — see text
P vapour pressure (kPa)
Q heat-flow rate per unit area of body surface; except for Q_D and Q_d, which refer to unit area of horizontal surfaces (W/m^2)
R resistance to heat transfer of unit area (m^2K/W)
T temperature (°C)
Z resistance of unit area to moisture transfer (m^2kPa/W)
v_{10} wind speed averaged over one minute, measured 10 m above ground (m/s)
AT apparent temperature; subscripts p, pv and pvg refer to effects of humidity alone; of humidity and wind; and to all effects, respectively
ϕ_1 ratio of body's effective radiating area to total surface area
ϕ_2 proportion of body surface covered by apparel
ϕ_3 ratio of body's projected area to effective radiating area
ϕ_4 fraction of sky covered by cloud
ϕ_5 fraction of global solar radiation that is direct
ε relative humidity

Subscripts

a ambient conditions; surface layer of air
b body core
c by convection
D & d direct and diffuse radiation on horizontal surface
f clothing; at outer surface of clothing
g due to nett extra radiation
n normally incident
r by radiation
s skin tissue; at surface of skin
′ clothed parts of human skin
v other than by breathing